

# Mark-Recapture with Multiple Non-invasive Marks

Simon Bonner and Jason Holmberg

May 22, 2022

## 1 **Abstract**

2 Non-invasive marks including pigmentation patterns, acquired scars, and  
3 genetic markers, are often used to identify individuals in mark-recapture experiments.  
4 Such data present new statistical challenges including that the marks  
5 may change over time, that the marks may be misidentified at non-negligible  
6 rates, and that only part of the population may possess a specific mark. Moti-  
7 vated by the analysis of data from the ECOCEAN online whale shark catalog,  
8 we consider issues that arise when individuals may be identified from multi-  
9 ple, non-invasive marks. Past approaches to this problem include modeling  
10 data from only one mark and combining inferences obtained from each mark  
11 separately under the assumption that marks are independent. We describe a  
12 Bayesian method that makes use of the data from multiple marks and properly  
13 accounts for the dependence between marks from the same individual. Results  
14 from the analysis of the ECOCEAN data and simulation studies are included  
15 and show that the new method provides more precise inference than analyzing  
16 the data from one mark while maintaining nominal coverage rates for credible  
17 intervals.

18 **Keywords:** Latent multinomial model; Mark-recapture; Multiple marks; Non-invasive  
19 marks; Photo-identification; Whale sharks

<sup>20</sup> **1 Introduction**

<sup>21</sup> Non-invasive marks (also called natural marks) include patterns in pigmentation, ge-  
<sup>22</sup> netic markers, acquired scars, or other natural characteristics that allow researchers  
<sup>23</sup> to identify individuals in a population without physical capture. Such marks have  
<sup>24</sup> been used for a long time in mark-recapture studies of some classes of animals, par-  
<sup>25</sup> ticularly marine mammals, and are now being used more widely. The advantages of  
<sup>26</sup> non-invasive marks over man-made marks are first that non-invasive marks can be ob-  
<sup>27</sup> served passively from a distance or through the collection of secondary material (hair  
<sup>28</sup> samples or scat) so that individuals do not have to be handled and second, depending  
<sup>29</sup> on the type of mark, that every individual is marked from birth. However, non-  
<sup>30</sup> invasive marks also present several modeling challenges including that marks may be  
<sup>31</sup> misidentified at non-negligible rates, that individuals' marks may change over time,  
<sup>32</sup> and that certain types of marks may be restricted to a subset of the population. We  
<sup>33</sup> consider the problem of modeling about the demographics of a population based on  
<sup>34</sup> mark-recapture data when individuals may be identified from multiple non-invasive  
<sup>35</sup> marks.

<sup>36</sup> The specific application we consider concerns the aggregation of whale sharks in  
<sup>37</sup> Ningaloo Marine Park (NMP), off the west coast of Australia, each year between April  
<sup>38</sup> and July. During this time, individual whale sharks are located by tour companies and  
<sup>39</sup> photographs are taken by tourists and tour operators who upload their images to the  
<sup>40</sup> online ECOCEAN whale shark library. Whale sharks can be identified by the unique  
<sup>41</sup> pattern of spots on their flanks, and computer assisted methods are used to match  
<sup>42</sup> photographs in the library and generate capture histories which provide information  
<sup>43</sup> about the timing of the sharks' arrival and departure from NMP and their survival  
<sup>44</sup> across years (Holmberg et al., 2009). Yoshizaki et al. (2009) and Yoshizaki et al.

45 (2011) list many more applications involving the use of non-invasive marks with wide  
46 range of species including photographs of large cats (cheetahs, snow leopards, and  
47 tigers), scar patterns on marine mammals (manatees and whales), skin patterns of  
48 reptiles and amphibians (snakes, crocodiles, and salamanders), and genetic marks  
49 (bears, wombats, and whales).

50 Though non-invasive marks provide advantages they also present modeling chal-  
51 lenges that do not arise with man-made tags. Da-Silva et al. (2003) and Da-Silva  
52 (2006) consider difficulties that occur if only a portion of the population possesses  
53 the non-invasive mark; for example, if individuals are identified from body scars that  
54 they acquire over time. Some individuals are effectively uncatchable because they  
55 cannot be identified, and abundance estimates must be inflated to account for this  
56 portion of the population. A related challenge is that non-invasive marks may change  
57 over time, as individuals acquire new scars or their skin patterns change. Yoshizaki  
58 et al. (2011) calls these as “evolving marks” and develops a least squares based method  
59 that allows for estimation of population demographics under the assumption that it is  
60 impossible to match the mark before and after the change creating a “ghost capture  
61 history” (Yoshizaki et al., 2011, pg. 29).

62 Work has also been done on the problem of misidentification of non-invasive marks,  
63 particularly for genetic marks. Lukacs and Burnham (2005) develops an extension of  
64 the Jolly-Seber model to account for misidentification of genetic markers under the  
65 assumption that the same error cannot occur twice and that errors do not produce  
66 spurious matches with other individuals. This produces an apparent excess of indi-  
67 viduals captured once from which the rate of misidentification is estimated. Yoshizaki  
68 et al. (2011) shows that the estimators of Lukacs and Burnham (2005) are biased,  
69 even in large samples, and presents an alternative least squares approach based on  
70 the same assumptions. Further, Wright et al. (2009) presents a method that relaxes

71 the assumptions that errors in identification when the probability that markers are  
72 misread can be estimated from multiple tests of each genetic sample.

73 The problem we address arises when a single individual can be identified from  
74 more than one non-invasive mark, but the marks are not always linked. This occurs  
75 in our example because a single whale shark may be photographed from either the right  
76 or the left side, but the spot patterns on each side are distinct and cannot be linked  
77 without further information. This means that it may not be possible to connect ob-  
78 servations of a shark photographed one from the left and later from the right and to  
79 know that the same individual was in fact encountered twice. Naively modeling the  
80 observed encounter histories will artificially inflate the number of individuals observed  
81 and create dependence between the encounter histories, violating a key assumption of  
82 most mark-recapture models. One solution is to construct encounter histories from a  
83 single mark, Holmberg et al. (2009) considers only left-side photographs, but this may  
84 remove a large number of histories from the data. Alternatively, Wilson et al. (1999)  
85 combines inferences from each mark *post hoc* by averaging separates estimates of abun-  
86 dance and computing standard errors under the assumption that these estimates are  
87 independent. It is simple to show that the final point estimate has similar properties  
88 to the individual estimates – the overall estimate will be unbiased/consistent if each of  
89 the separate estimates is unbiased/consistent – but the assumption of independence  
90 is violated and the resulting standard errors will be biased low. Madon et al. (2011)  
91 describes another method to estimate abundance by adjusting the sufficient statistics  
92 required to compute the Jolly-Seber estimator. While the approach seems plausible,  
93 we have concerns with the implementation; though the observed counts underesti-  
94 mate some of the statistics and overestimate others, Madon et al. (2011) uses a single  
95 adjustment factor and constrains its value to be between 0 and 1. Bonner (2012)  
96 discusses these issues and shows that the correct adjustment factor is not constant

97 and may be greater than 1 for some statistics. Moreover, the simulations Madon et al.  
98 (2011) presents indicate a clear problem in that the coverage of confidence intervals  
99 is much lower than their nominal value, even when the population is large and the  
100 capture probability is close to 1.

101 Our objectives are to construct a model that accounts for the dependence between  
102 multiple non-invasive marks and provides valid inference about the population's de-  
103 mographics while making use of all available data. We do so by constructing an  
104 explicit model of the observation process that allows for multiple marks to be ob-  
105 served on different occasions and then applying Bayesian methods of inference via  
106 Markov chain Monte Carlo (MCM) sampling. Our model can be cast as a special  
107 case of the latent multinomial model (LMM) of Link et al. (2010). Section 2 describes  
108 the whale shark data and Section 3 gives details on the structure of our model and  
109 our methods of inference. We provide results from a simulation study and the appli-  
110 cation of our method to the whale shark data in Sections 4 and 5, and conclude with  
111 a discussion of the method and further extensions in Section 6.

## 112 2 Data

113 Data for our analysis was obtained from the ECOCEAN on-line whale shark library  
114 (available at [www.whaleshark.org](http://www.whaleshark.org)). This library contains photographs of whale  
115 sharks taken by recreational divers and tour operators worldwide and submitted on-  
116 line. Computer assisted algorithms are then used to identify the pattern of spots  
117 on the shark's flank and scan the database for matches with previous photographs  
118 which are confirmed visually. Quality control studies indicated that the probability  
119 of a mismatch is approximately .02 (Holmberg et al., 2009). The library has been  
120 operational since 2003, and over 41,000 photographs have been submitted by more

121 than 3300 contributors. Further details on the study site, the observation protocols,  
122 and the algorithms for matching photographs are provided in Holmberg et al. (2009).

123 We model only the data collected from the northern ecotourism zone of NMP  
124 during the 16 week period between April 1 and July 31, 2008, which we have divided  
125 into 8 capture periods of 2 weeks each. Sharks may be encountered multiple times  
126 during a single capture period and so five possible events may occur. In each 2 week  
127 period, a shark may:

- 128 1) not be encountered at all (event 0)
- 129 2) be photographed from the left only (event L),
- 130 3) be photographed from the right only (event R),
- 131 4) be photographed from both sides simultaneously on at least one encounter (event  
132 S), or
- 133 5) be photographed from both sides but never simultaneously (event B).

134 Problems with identification arise because it is only possible to match the skin pat-  
135 terns from the two sides of a shark if photographs of both sides are taken simultane-  
136 ously during at least one capture period – i.e., there is at least one S in its encounter  
137 history. Otherwise, an individual that was photographed from both sides will con-  
138 tribute two encounter histories to the data set – one containing the observations of  
139 its right side and the other containing the observations of its left side.

<sup>140</sup> **3 Methods**

<sup>141</sup> **3.1 Modeling**

<sup>142</sup> The challenge in modeling this data is that some encounter histories are unobservable  
<sup>143</sup> so that the recorded histories may not reflect the true histories of the encountered  
<sup>144</sup> individuals. Suppose that an individual's true encounter history is 00L0B0R0. This  
<sup>145</sup> history is not observable because the two sides of the individual were never pho-  
<sup>146</sup> tographed simultaneously and the marks on its right and left sides cannot be linked.  
<sup>147</sup> Instead, the individual will contribute two observed histories to the data – 00L0L000  
<sup>148</sup> and 0000R0R0. Working in the opposite direction, if the observed data includes the  
<sup>149</sup> histories 00L0L000 and 0000R0R0 then it is not possible to know if these histories  
<sup>150</sup> come from one individual encountered on three occasions or from two individuals  
<sup>151</sup> encountered twice each.

<sup>152</sup> With  $K = 8$  capture occasions there are  $5^8 - 1 = 390,624$  possible true encounter  
<sup>153</sup> histories (we ignore the zero history because our model conditions on an individual  
<sup>154</sup> being captured once at least). Of these, 325,558 (83.3%) can occur in the observed  
<sup>155</sup> data because they contain photographs from the left-side only, photographs from the  
<sup>156</sup> right-side only, or at least one simultaneous encounter. The remaining 65,026 (16.7%)  
<sup>157</sup> contain photographs taken from both the left and right sides, including via event B,  
<sup>158</sup> but never simultaneously and are unobservable. In practice, we need not consider  
<sup>159</sup> all 65,026 unobservable histories. Given a set of observed histories, the possible  
<sup>160</sup> true histories can be constructed by combining each history containing only left-  
<sup>161</sup> side photographs with each history containing only right-side photographs as follows:  
<sup>162</sup> when event L appears in the first history and 0 appears in the second enter L in the  
<sup>163</sup> combined history, when 0 appears in the first history and R in the second enter R in  
<sup>164</sup> the combined history, and when L appears in the first and R in the second then B is

165 entered into the combined history.

166 To account for the uncertainty in the true encounter histories when modeling the  
167 demographics of the population we adapt the LMM of Link et al. (2010). This model  
168 applies when the latent counts of the true histories follow a multinomial distribution  
169 and determine the observed counts through a known, linear relationship. Suppose  
170 that  $L$  unique histories were observed, let  $n_j$  be the number of times that the  $j^{th}$   
171 history was observed, and set  $\mathbf{n} = (n_1, \dots, n_L)^T$ . Further, suppose that there are  
172  $L^*$  true histories that could have generated the observed histories, let  $n^*j$  be the  
173 number of individuals with the  $j^{th}$  true history, and set  $\mathbf{n}^* = (n_1^*, \dots, n_{L^*}^*)^T$ . The  
174 LMM supposes first that  $\mathbf{n} = \mathbf{A}\mathbf{n}^*$  for some fixed matrix  $\mathbf{A}$  and second that  $\mathbf{n}^*$  has  
175 a multinomial distribution whose density,  $f(\mathbf{n}^*|n^*, \boldsymbol{\theta})$ , depends on  $n^*$ , representing  
176 either the total population size or the number of unique individuals encountered,  
177 and the vector of parameters  $\boldsymbol{\theta}$ . The likelihood for this model is proportional to the  
178 probability of  $\mathbf{n}$  given both  $n^*$  and  $\boldsymbol{\theta}$  and is computed by summing  $f(\mathbf{n}^*|n^*, \boldsymbol{\theta})$  over  
179 all possible configurations of  $\mathbf{n}^*$  that satisfy equation (??) and produce the correct  
180 value of  $n^*$  ( $n^* = \sum n_j^*$ ). Evaluating this sum directly is generally not possible, and,  
181 instead, Link et al. (2010) applies Bayesian inference treating  $\mathbf{n}^*$  as a random variable  
182 and sampling from the joint posterior distribution

$$\pi(\mathbf{n}^*, n^*, \boldsymbol{\theta} | \mathbf{n}) \propto 1(\mathbf{n} = \mathbf{A}\mathbf{n}^*) f(\mathbf{n}^*|n^*, \boldsymbol{\theta}) \pi(n^*, \boldsymbol{\theta}) \quad (1)$$

183 where  $\pi(n^*, \boldsymbol{\theta})$  is the chosen prior for  $n^*$  and  $\boldsymbol{\theta}$ .

184 To apply the LMM to our problem, we need to identify the set of possible true  
185 histories that could have generated the observed data and the relationship between  
186 the corresponding counts. Suppose that the observed data contains  $L_1$  unique histo-  
187 ries including only left-side photographs,  $L_2$  unique histories including only right-side

188 photographs, and  $L_3$  unique histories with at least one encounter of both sides simultaneously so that  $L = L_1 + L_2 + L_3$ . Let  $\mathbf{W}_1$  be the  $L_1 \times K$  matrix whose rows contains  
 189 those histories including only left-side photographs and  $\mathbf{n}_1$  the  $L_1$ -vector of observed  
 190 counts for each row of  $\mathbf{W}_1$ . Define  $\mathbf{W}_2$ ,  $\mathbf{n}_2$  and  $\mathbf{W}_3$ ,  $\mathbf{n}_3$  similarly for those histories  
 191 including only right side photographs and those including at least one simultaneous  
 192 encounter so that the complete vector of observed counts is  $\mathbf{n} = (\mathbf{n}_1^T, \mathbf{n}_2^T, \mathbf{n}_3^T)^T$ .  
 193 The additional entries in the set of possible true histories are then generated by com-  
 194 bining each row of  $\mathbf{W}_1$  with each row of  $\mathbf{W}_2$ , as described above. Let  $\mathbf{W}_4$  denote  
 195 the  $L_4 \times K$  matrix of unobservable histories ( $L_4 = L_1 L_2$ ) whose  $L_1(i-1) + j$  row is  
 196 formed by combining row  $i$  of  $\mathbf{W}_1$  with row  $j$  of  $\mathbf{W}_2$ . Let  $n_{4ij}^*$  denote the number of  
 197 individuals encountered whose true encounter history given by the  $L_1(i-1) + j^{th}$  row  
 198 of  $\mathbf{W}_4$  and  $\mathbf{n}_4^* = (n_{411}^*, \dots, n_{4L_11}^*, \dots, n_{41L_2}^*, \dots, n_{4L_1L_2}^*)^T$  so that the complete vector  
 199 of true counts is  $\mathbf{n}^* = (\mathbf{n}_1^{*T}, \mathbf{n}_2^{*T}, \mathbf{n}_3^{*T}, \mathbf{n}_4^{*T})^T$ .  
 200

201 The set of linear constraints mapping  $\mathbf{n}^*$  to  $\mathbf{n}$  is then obtained by considering  
 202 how each true history contributes to each observed history. Specifically, the number  
 203 of times that a history in  $\mathbf{W}_1$  or  $\mathbf{W}_2$ , say  $\mathbf{w}$ , is observed must equal the sum of the  
 204 counts for all of the true histories that could have generated  $\mathbf{w}$ . These constraints  
 205 are determined by the set of  $L$  linear equations

$$\begin{aligned}
 n_{1i} &= n_{1i}^* + \sum_{j=1}^{L_2} n_{4ij}^*, \quad i = 1, \dots, L_1 \\
 n_{2j} &= n_{2j}^* + \sum_{i=1}^{L_1} n_{4ij}^*, \quad j = 1, \dots, L_2 \\
 n_{3k} &= n_{3kj}^*, \quad k = 1, \dots, L_3
 \end{aligned} \tag{2}$$

206 one for each observed history. Note that there are  $L$  equations and  $L^*$  unknowns,  
 207 implying that there are  $L^* - L = L_4^*$  free parameters. It is most convenient to choose

208  $\mathbf{n}_4^*$  as the set of free parameters, and the possible values can be bounded by noting  
 209 that  $0 \leq n_{4ij}^* \leq \min(n_{1i}, n_{2j})$ . This limits the possible configurations of  $\mathbf{n}_4^*$  and makes  
 210 it easier to sample from the posterior distribution, as described in Section 3.3.

211 As an example, suppose that the observed data comprises the six histories listed  
 212 in the top of Table 1. The possible true histories that generated this data include  
 213 the six observed histories plus the four unobservable histories generated by combining  
 214 the histories including only of left-side photographs (histories 1&2) with the histo-  
 215 ries including only right-side photographs (histories 3&4), as given in the bottom of  
 216 the table. The relationship between  $\mathbf{n}$  and  $\mathbf{n}^*$  is then determined by the six linear  
 217 equations

$$\begin{aligned} n_1 &= n_1^* + n_7^* + n_9^*, & n_3 &= n_3^* + n_7^* + n_8^*, & n_5 &= n_5^* \\ n_2 &= n_2^* + n_8^* + n_{10}^*, & n_4 &= n_4^* + n_9^* + n_{10}^*, & n_6 &= n_6^*. \end{aligned}$$

218 The free parameters are  $n_7^*, \dots, n_{10}^*$  and these values are bounded so that  $0 \leq n_7^* \leq$   
 219  $\min(n_1, n_3)$ ,  $0 \leq n_8^* \leq \min(n_2, n_3)$ ,  $0 \leq n_9^* \leq \min(n_1, n_4)$ , and  $0 \leq n_{10}^* \leq \min(n_2, n_4)$ .

220 [Table 1 about here.]

## 221 3.2 Model of Observed Encounter Histories

222 This framework for modeling data from multiple non-invasive marks is general and  
 223 can incorporate any of the standard mark-recapture models for the true encounter  
 224 histories. We are most interested in the timing of the sharks' arrival and departure  
 225 from NMP and have developed an extension of the Link-Barker-Jolly-Seber (LBJS)  
 226 model (Link and Barker, 2005) which accounts for the presence of multiple marks.  
 227 The LBJS model describes the demographics of a population through two sets of

parameters: 1) the recruitment rate,  $f_k$ ,  $k = 1, \dots, K - 1$ , defined as the number of individuals that enter the population between occasions  $k$  and  $k + 1$  per individual present on occasion  $k$  and 2) the survival probability,  $\phi_k$ ,  $k = 1, \dots, K - 1$ , defined as the probability that an individual present on occasion  $k$  is also present on occasion  $k + 1$ . For the whale sharks,  $\phi_k$  corresponds to the probability that an individual remains at NMP rather than true survival. It is assumed that all emigration is permanent, that individuals behave independently, and that the apparent survival probability does not depend on how long an individual has been present (or any other factors).

The process of observing individuals is then modeled in terms of two further sets of parameters: 1) the probability that an individual is captured/encountered given that it is present in the study area and 2) the conditional probabilities of each event. Specifically, we define  $p_k$  to be the probability that an individual is photographed at least one time during occasion  $k$  given that it is present,  $k = 1, \dots, K$ , and  $\rho_j$  to be the probability that the individual is photographed from the left-side only ( $j = 1$ ), from the right-side only ( $j = 2$ ), from both sides simultaneously at least once ( $j = 3$ ), or from both sides but never simultaneously ( $j = 4$ ) during period  $k$ . This last set of parameters is what distinguishes our model of the true histories from the original model of Link and Barker (2005). Our model assumes that all individuals present on an occasion have the same probability of capture, that encounters are independent between individuals and across the occasions, and that the conditional event probabilities do not vary between individuals or over time.

250 **3.3 Inference**

251 As noted by Link et al. (2010), the LMM lends itself to Bayesian inference via MCMC  
252 sampling with data augmentation, and the Bayesian specification of the model is com-  
253 pleted by assigning prior distributions to all of the parameters. We have selected non-  
254 informative, hierarchical prior distributions where possible. Specifically, the survival  
255 and capture probabilities were assigned prior distributions

$$\text{logit}(\phi_k) \sim N(\mu_\phi, \sigma_\phi^2), \quad k = 1, \dots, K - 1$$

$$\text{logit}(p_k) \sim N(\mu_p, \sigma_p^2), \quad k = 1, \dots, K$$

256 with

$$\mu_\phi, \mu_p \sim N(0, 2) \text{ and } \sigma_\phi, \sigma_p \sim HT(3, .9)$$

257 where  $HT$  denotes the half  $t$ -distribution with 3 degrees of freedom and scale pa-  
258 rameter .9. These hyperparameters were chosen because they provide distributions  
259 that are close to uniform on  $(0, 1)$  for both the hierarchical means,  $\mu_\phi$  and  $\mu_p$ , and  
260 the base demographic parameters,  $\phi_k$  and  $p_k$ . The recruitment probabilities were  
261 assigned prior distributions of the form

$$\log(f_k) \sim N(\mu_f, \sigma_f^2), \quad k = 1, \dots, K - 1$$

262 with

$$\mu_f \sim N(0, .25) \text{ and } \sigma_f \sim HT(3, .9),$$

263 and the number of unique individuals encountered was assigned the discrete uni-  
264 form prior on  $0, \dots, M$  for some  $M$  guaranteed not to be smaller than  $n^*$ . This  
265 is satisfied by the data dependent prior  $n^* \sim U\{0, \dots, L_1 + L_2 + L_3\}$ , because

266  $n^* = \sum_{j=1}^{L^*} n_j^* \leq \sum_{j=1}^L n_j$ , but the exact value does not affect our computations.

267 Finally, the conditional event probabilities were assigned a Dirichlet prior with  
 268 parameter  $\alpha = \mathbf{1}_4$  implying that  $\rho_1, \rho_2, \rho_3$ , and  $\rho_4$  were marginally distributed *a priori*  
 269 with identical beta distributions having mean .25 and probability .9 between .00 and  
 270 .86. All prior distributions were assumed independent.

271 An MCMC algorithm for sampling from the distribution in (1) can then be im-  
 272 plemented as follows. Letting  $\mathbf{n}^{*(k)}$ ,  $n^{*(k)}$ , and  $\boldsymbol{\theta}^{(k)}$ , denote the values sampled on the  
 273  $k^{th}$  iteration, the values on the next iteration are generated in two steps:

274 1. Update  $\mathbf{n}^{*(k)}$  and  $n^{*(k)}$  given  $\boldsymbol{\theta}^{(k)}$  by:

275 a) setting  $\mathbf{n}^{*(curr)} = \mathbf{n}^{*(k)}$  and  $n^{*(curr)} = n^{*(k)}$ ,

276 b) updating  $n_{411}^*$  by:

277 i) setting  $\mathbf{n}^{*' = \mathbf{n}^{*(curr)}}$

278 ii) sampling a new value for  $n_{411}^{*'}$  from  $\{0, \dots, \min(n_{11}, n_{21})\}$  according to some  
 279 proposal distribution,  $q(n_{411}^* | \mathbf{n}^{*(curr)}, \boldsymbol{\theta}^{(k)})$ ,

280 iii) ensuring the constraints in equation (2) remain satisfied by setting

$$n_{11}^{*' = n_1 - \sum_{j=1}^{L_2} n_{41j}^*,} \\ n_{21}^{*' = n_2 - \sum_{i=1}^{L_1} n_{4i1}^*, \text{ and}} \\ n^{*' = \mathbf{1}^T \mathbf{n}^{*' = \mathbf{n}^{*(curr)}}},$$

281 iv) rejecting  $\mathbf{n}^{*'}$  if  $n_{11}^{*' < 0}$  or  $n_{21}^{*' < 0}$  and otherwise accepting  $\mathbf{n}^{*'}$  and setting  
 282  $\mathbf{n}^{*(curr)} = \mathbf{n}^{*'}$  and  $n^{*(curr)} = n^{*'}$  with probability:

$$\alpha(\mathbf{n}^*, \mathbf{n}^{*'}) = \min \left\{ 1, \frac{f(\mathbf{n}^{*' | n^{*' = \mathbf{n}^{*(curr)}}, \boldsymbol{\theta}^{(k)}) q(n_{411}^{*(curr)} | \mathbf{n}^{*' = \mathbf{n}^{*(curr)}}, \boldsymbol{\theta}^{(k)})}}{f(\mathbf{n}^{*(curr)} | n^{*(curr)}, \boldsymbol{\theta}^{(k)}) q(n_{411}^* | \mathbf{n}^{*(curr)}, \boldsymbol{\theta}^{(k)})} \right\}$$

283       c) repeating step b) for each  $n_{4ij}^*$ ,  $i = 1, \dots, L_1$ ,  $j = 1, \dots, L_2$ , and finally

284       d) setting  $\mathbf{n}^{*(k+1)} = \mathbf{n}^{*(\text{curr})}$  and  $n^{*(k+1)} = n^{*(\text{curr})}$ .

285       2. Update  $\boldsymbol{\theta}^{(k)}$  given  $\mathbf{n}^{*(k+1)}$  and  $n^{*(k+1)}$  through a series of Metropolis-Hastings (MH)  
286       steps appropriate for the selected model.

287       The steps for updating each element of  $\mathbf{n}^*$  in this algorithm have an intuitive inter-  
288       pretation. In step i), a new count is proposed for one of the unobservable histories.

289       In step ii), the counts of the corresponding observed histories in  $\mathbf{W}_1$  and  $\mathbf{W}_2$  are ad-  
290       justed to maintain the correct observed counts. The new proposal is rejected immedi-  
291       ately if this produces negative counts, and otherwise, a MH accept-reject step is con-  
292       ducted. One choice for  $q(n_{4ij}^* | \mathbf{n}^*, \boldsymbol{\theta})$  is the discrete uniform on  $\{0, \dots, \min(n_{1i}, n_{2j})\}$   
293       in which case the proposal,  $\mathbf{n}^{*'}$  is accepted whenever the likelihood is increased,  
294        $f(\mathbf{n}^{*'} | n^{*'}, \boldsymbol{\theta}) > f(\mathbf{n}^{*(\text{curr})} | n^{*(\text{curr})}, \boldsymbol{\theta})$ .

295       This MCMC sampling algorithm was implemented in JAGS using the rjags in-  
296       terface to the R software package (Plummer, 2003, 2011; Team, 2012). Three chains  
297       were run in parallel in order that convergence could be monitored with the Gelman-  
298       Rubin-Brooks (GRB) diagnostic (Brooks and Gelman, 1998) as implemented in the  
299       R package CODA (Plummer et al., 2006). One challenge we faced was obtaining  
300       initial values for different sets of parameters were dispersed but consistent with one  
301       other. To do this, we generated initial values for each chain in three steps. First, we  
302       simulated random values of  $\phi_k$  and  $f_k$ ,  $k = 1, \dots, K - 1$ , under one of three schemes –  
303       1)  $\text{logit}(\phi_k) \sim N(\text{logit}(.9), .1)$  and  $\log(f) \sim N(\log(.1), .1)$ , 2)  $\text{logit}(\phi_k) \sim N(., .1)$  and  
304        $\log(f) \sim N(\log(.5), .9)$ , 3)  $\text{logit}(\phi_k) \sim N(\text{logit}(.1), .1)$  and  $\log(f) \sim N(\log(.9), .1)$ .  
305       We then obtained values of  $p_k$ ,  $k = 1, \dots, K$ , by fitting the LBJS model to the  
306       data obtained from the left-side photographs only but treating the sampled values  
307       of  $\phi_k$  and  $f_k$  as fixed. Finally, we obtained values of  $\mathbf{n}^*$  by fitting the our model

308 to the full data set but treating all of  $\phi_k$ ,  $f_k$ , and  $p_k$  as fixed. An R package which  
309 implements these methods and provides functions to format the data and to call  
310 JAGS through the rjags interface is available from the website of the first author at  
311 [www.simon.bonners.ca/MultiMark](http://www.simon.bonners.ca/MultiMark).

## 312 4 Simulation Study

313 To assess the performance of the model presented in the previous section we conducted  
314 simulation studies under a variety of scenarios. Here we present the results from three  
315 simulation scenarios which illustrate our main results.

316 In the first scenario, we compared the performance of the new model (henceforth  
317 the two-sided model) with two alternative models. First, we considered models using  
318 reduced data sets containing only data from the left or right side photographs (the  
319 one-sided models). Capture histories were constructed by combining all events that  
320 include a left-side photograph, namely L, S, and B, and all right-side photographs  
321 were ignored, or vice versa. The models we fit to this data were equivalent to the  
322 LBJS model with prior distributions as given in Section 3.3. Second, we developed a  
323 Bayesian equivalent of the method of combining inferences from the two sides under  
324 the assumption of independence as in (Wilson et al., 1999) (combined inference). To  
325 do this, we fit separate models to the data from the left and right side photographs and  
326 then averaged the values sampled on each iteration of the separate MCMC samplers  
327 prior to computing summary statistics. For example, let  $\phi_t^{(k,L)}$  and  $\phi_t^{(k,R)}$  represent  
328 the values of  $\phi_t$  drawn on the  $k^{th}$  iterations of the MCMC samplers run separately for  
329 models of the the left and right-side data and  $\text{Var}^{(L)}(\phi_t)$  and  $\text{Var}^{(R)}(\phi_t)$  be the separate  
330 posterior variances. Combined inference for  $\phi_t$  was obtained by first computing the

331 inverse variance weighted average of the samples drawn on the  $k^{th}$  iteration

$$\phi_t^{(k)} = \frac{(\text{Var}^{(R)}(\phi_t)\phi_t^{(k,L)} + \text{Var}^{(L)}(\phi_t)\phi_t^{(k,R)})}{\text{Var}^{(L)}(\phi_t) + \text{Var}^{(R)}(\phi_t)}$$

332 and then computing summary statistics from the new chain  $\phi_t^{(1)}, \phi_t^{(2)}, \dots$ . The ad-  
333 vantage of this method is that posterior standard deviations and credible intervals  
334 can be computed directly from the new chain without distributional assumptions.  
335 Note that the mean of the values in the new chain is exactly equal to the inverse  
336 variance weighted average of means from the separate chains. We expected that, in  
337 general, posterior standard deviations and credible intervals from the one-sided mod-  
338 els would be larger/wider than the corresponding standard deviations and intervals  
339 from the two-sided model, and that posterior standard deviations and credible inter-  
340 vals produced by combined inference would be smaller/narrower than those from the  
341 two-sided model but would not achieve the nominal coverage probability.

342 One hundred data sets for this scenario were generated under the assumption that  
343 each event was equally likely conditional on capture ( $\rho_1 = \rho_2 = \rho_3 = \rho_4 = .25$ ). Sim-  
344 ulated capture histories included 10 capture occasions, and data were generated by  
345 simulating true capture histories for individuals sequentially until 200 observed cap-  
346 ture histories were produced (each true history contributing either 0, 1, or 2 histories  
347 to the observed data). Survival and capture probabilities for each occasion were gen-  
348 erated from independent logit-normal distributions with means  $\text{logit}(.8)$  and  $\text{logit}(.5)$ ,  
349 and standard deviation .30. Recruitment rates were generated from independent log-  
350 normal distributions with mean  $\log(.25)$  and standard deviation .30. The median  
351 number of true histories simulated before 200 observed histories were obtained was  
352 164 (min=150,max=180), the median number of unique individuals observed at least  
353 one time was 138 (min=127,max=148), and the median number of captures was 2

354 (min=1,max=10).

355 Table 2 presents statistics comparing the mean-squared error (MSE) of the pos-  
356 terior means and the mean width and estimated coverage probability of the 95%  
357 credible intervals obtained from the alternative models. The MSE of the two-sided  
358 model and the combined-inference were similar for all parameters and smaller than  
359 those of the one-sided model by between 10% and 25%. Credible intervals for both  
360 the one-sided and two-sided model achieved the nominal coverage rate for all param-  
361 eters, but the credible intervals for the one-sided model were wider by approximately  
362 10%. In comparison, the credible intervals from the combined inference were narrower  
363 than those of the two-sided model by 20% or more but failed to achieve the nominal  
364 coverage rate.

365 In the second scenario, we simulated data under the same model except that  
366 the capture probabilities were generated from a logit-normal distribution with mean  
367  $\text{logit}(.5)$ . The result is that capture probabilities were lowered and the number of  
368 observations per individual decreased. From the 100 data sets generated, the median  
369 number of true histories simulated before 200 observed histories were obtained was 196  
370 (min=170,max=235), the median number of unique individuals observed at least one  
371 time was 131 (min=119,max=143), and the median number of captures per observed  
372 individual was 1 (min=1,max=9). In this scenario, the MSEs of the posterior mean  
373 survival probabilities was similar between the two-sided model and the combined  
374 inference, but the two-sided model produced higher MSEs for both the recruitment  
375 and population growth rates. Credible intervals from the two-sided model were again  
376 narrower than those of the one-sided model by approximately 10%, but coverage  
377 probabilities from both models were above the nominal rate. Finally, although the  
378 credible intervals from the combined inference were narrower than those of the two-  
379 sided model by approximately 20%, the coverage of these intervals was also increased

380 and was near or above the nominal value. This result was due to the combination  
381 of non-informative priors and the relatively small amount of information in the data  
382 when capture probabilities are low; we discuss this point in Section 6

383 In the third scenario, we simulated data from the same model used in the first  
384 scenario except that both marks were seen with probability one each time an indi-  
385 vidual was captured ( $\rho_3 = 1$ ). This represents the extreme situation in which there is  
386 complete dependence between the two marks and no uncertainty in the true capture  
387 histories. Modeling the data from the left-side photographs, right-side photographs,  
388 or from both-sides using our model produces exactly the same results, and so we only  
389 compare the model of the left-side photographs with combined inference. The me-  
390 dian number of histories simulated in the 100 data sets before 200 observed histories  
391 were obtained was 215 (min=204,max=227) and the median number of captures per  
392 observed individual was 2 (min=1,max=10). In this scenario, the point estimates  
393 produced by the two models were almost exactly equal and the MSE of the two mod-  
394 els was indistinguishable. However, there were clear differences in the performance of  
395 the 95% credible intervals. While the intervals produced by combined-inference were,  
396 on average, 30% narrower the coverage of these intervals was well below the nominal  
397 value.

398 [Table 2 about here.]

## 399 5 Results

400 The data provided in the ECOCEAN whale shark library contained a total of 96  
401 observed encounter histories for the 2008 study period. Of these, 27 histories (28%)  
402 were constructed from left-side photographs alone, 24 (25%) were constructed from  
403 right-side photographs alone, and 45 (47%) contained at least one encounter with

404 photographs taken from both sides simultaneously. Along with the model presented  
405 in Section 3, we computed inferences for  $\mathbf{p}$ ,  $\mathbf{f}$ , and  $\phi$  from the three alternative models  
406 described in Section 4.

407 Table 3 provides posterior summary statistics for the LBJS parameters model  
408 obtained from the two-sided model. Inferences about all parameters are relatively  
409 imprecise because of the relatively small number of individuals captured and the low  
410 capture probabilities, but the posterior means follow the expected patterns. Point  
411 estimates for the survival probability (the probability that a whale shark remains  
412 NMP between occasions) are at or above .90 in the first 2 periods, below .70 in the  
413 last two periods, and about .80 in between. The posterior mean recruitment rate is  
414 very high in week 2, suggesting that most of the sharks entered during this period,  
415 and lower thereafter. This table also provides summary statistics for the population  
416 growth rate,  $\lambda_k = \phi_k + f_k$ ,  $k = 1, \dots, K - 1$ , computed as a derived parameter.  
417 Although the 95% credible intervals for  $\lambda_k$  cover 1.00 for all  $k$ , the point estimates  
418 are greater than 1.00 for the first two periods, close to 1.00 in the next three periods,  
419 and less than .75 in the last two periods. This suggests that the aggregation of whale  
420 sharks grew during the first two periods, remained almost steady during the next 3  
421 periods, and declined during the last two periods. This supports the hypothesis that  
422 whale sharks aggregate at NMP to feed after the major coral spawn which occurred  
423 between April 9 and 12 in 2008 (Chalmers, 2008, pg. 33).

424 [Table 3 about here.]

425 Table 4 provides posterior summary statistics for the conditional event probabili-  
426 ties. These results show that when sharks were encountered photographs were most  
427 often taken from both sides simultaneously ( $\hat{\rho}_3 = .45(.36, .54)$ ) and that the proba-  
428 bilities that an individual was photographed from either the left- or right-side only

429 were similar ( $\hat{\rho}_1 = .29(.20, .38)$  versus  $\hat{\rho}_2 = .21(.13, .29)$ ).

430 The posterior mean of  $n^*$ , the number of unique sharks encountered during the  
431 2008 season, was 88 with 95% credible interval (82,93). The full posterior distribution  
432 of  $n^*$  is shown in Figure 1 and compared with the prior distribution of  $n^*$  generated by  
433 simulating data sets from the prior predictive distribution conditional on there being  
434 96 observed capture histories and at least 72 true histories (the minimum number  
435 given that 24 of 96 observed histories included right-side photographs alone). Whereas  
436 the prior distribution of  $n^*$  is close to uniform the posterior distribution is strongly  
437 peaked and concentrates 95% of its mass between 82 and 93. We conclude that  
438 between 3 (3.1%) and 14 (14.6%) of the sharks encountered during the 2008 season  
439 were photographed from both the left- and right-sides on separate occasions without  
440 ever being matched.

441 [Table 4 about here.]

442 [Figure 1 about here.]

443 Comparisons of the three chains starting from different initial values provided  
444 no evidence of convergence problems. Traceplots all indicated that the three chains  
445 converged within the burn-in period, GRB diagnostic values were all less than 1.02,  
446 and the estimated MCMC error was less than 2.6% of the posterior standard deviation  
447 for each parameter. Based on these results, we are confident that the chains converged  
448 and were run for sufficiently long to obtain reliable summary statistics.

449 The plots in Figure 2 compare inferences for the survival, recruitment, and growth  
450 rates from the four alternative models. Posterior means from the four models are all  
451 very similar and the 95% credible intervals for all parameters overlap considerably.  
452 Comparison of the widths of the 95% credible intervals from the left- and right-side

453 data alone showed that the two-sided model provided improved inference in most,  
454 but not all, parameters. On average, the 95% credible intervals for the recruitment  
455 rates produced by the two-sided model were 93% and 69% as wide as those produced  
456 from the left- and right-side data alone. The 95% credible intervals for the survival  
457 probabilities produced by the two-sided model were 78% as wide as those from the  
458 right-side data, on average, but 103% as wide as those from the left-side data. This  
459 last result seems to be caused by issues with the upper bound on the survival prob-  
460 abilities as the 95% credible intervals for the logit transformed survival probabilities  
461 produced from the two-sided model were, on average, 90% and 89% as wide as those  
462 obtained from the left- and right-side data alone. Credible intervals produced via  
463 combined inference were on average 12% smaller than those obtained from the two-  
464 sided model; however, based on the results in the previous section, we believe that  
465 these intervals would not achieve the nominal coverage rate and do not reflect the  
466 variability of the parameters correctly.

467 [Figure 2 about here.]

## 468 6 Conclusion

469 The simulation results presented in Section 4 illustrate the main advantages of our  
470 model over the previous approaches to analyzing mark-recapture data with multiple  
471 non-invasive marks. In general, estimates from our model will be more precise than  
472 estimates based on only one mark in that posterior standard deviations will be smaller  
473 and credible intervals will be narrower but still achieve the nominal coverage rate.  
474 In contrast, the apparent gain from combining estimators computed separately for  
475 each mark under the assumption of independence is artificial and credible/confidence  
476 intervals computed by these methods will not achieve the nominal coverage rate –

477 particularly when the probability that both marks are seen simultaneously is high and  
478 the separate estimators are highly dependent. The differences between the methods  
479 are smaller when the capture probabilities are low (as in Simulation 2) but this is  
480 not surprising given that we have selected non-informative prior distributions. The  
481 posterior distribution is influenced more by the prior as the amount of information in  
482 the data decreases, and this would not have occurred if more informative priors had  
483 been selected.

484 The disadvantage of the two-sided model is that the computations are more com-  
485 plex and more time consuming. The major challenge is that the number of possible  
486 true capture histories grows relative to the square of the number of observed capture  
487 histories. Possible solutions include deriving more efficient methods of computation  
488 or approximating the posterior distribution in some way. Further research is needed  
489 in this area before applying our model to large data sets.

490 In the analysis of the whale shark data, we have focused on understanding the  
491 dynamics of the population (i.e., survival, recruitment, and population growths rates)  
492 but the method is easily adapted to estimate abundance. Following Link et al. (2010),  
493 one can include the null encounter history (vector of 0s) to the set of possible true  
494 histories and extend the vector of counts for the true histories to  $\mathbf{n}^* = (\mathbf{n}_1^*, \dots, \mathbf{n}_4^*, n_0^*)$   
495 where  $n_0^*$  represents the number of individuals in the population that were never  
496 captured. The value  $n^* = \mathbf{1}^T \mathbf{n}^*$  would then denote the total population size. Note  
497 that the prior on  $n^*$  must also be modified by increasing  $M$  to allow  $n^*$  to be larger  
498 than the number of observed histories.

499 Our model can also be extended to combine data from any number of marks  
500 by expanding the set of constraints, and we expect that including more marks will  
501 strengthen differences between the alternative methods seen in the simulation study.  
502 The ratio between the median width of the credible intervals from the one-sided model

503 and the combined inference is close to 1.4 for all parameters in all three simulation  
504 scenarios – very near the  $\sqrt{2}$  reduction in standard deviation that occurs when two  
505 identically distributed and perfectly correlated random variables are averaged. Gen-  
506 erally, posterior standard deviations computed under the assumption of independence  
507 should decrease relative to the square root of the number of marks used, but the gain  
508 is artificial and the coverage of credible/confidence intervals will decrease further be-  
509 low the nominal value as more marks are used. In comparison, our model will account  
510 for the dependence between marks and will provide more precise inference without  
511 sacrificing coverage.

512 One unusual aspect of the whale shark study is that individuals may be encoun-  
513 tered multiple times during each capture period. This would not occur if the capture  
514 periods were truly instantaneous, and in such cases both marks could only be observed  
515 in the same period if they were seen simultaneously. Event B could never occur. Our  
516 model could be fit to such data simply by specifying, *a priori*, that  $P(\rho_4 = 0) = 1$ .  
517 and other researchers have begun to develop similar methods specific to such data  
518 (Conn and McClintock, pers. comm.).

## 519 **Acknowledgments**

520 We thank Laura Cowen for providing comments on a previous draft of the manuscript  
521 and Matt Schofield for valuable discussions during the development of our model.  
522 Support for this work was provided in part by the NSF-Kentucky EPSCOR Grant  
523 (NSF Grant No. 0814194).

524 **References**

525 Bonner, S. J. (2012). Comment on: A new method for estimating animal abundance  
526 with two sources of data in capture-recapture studies. *Methods in Ecology and*  
527 *Evolution* Submitted.

528 Brooks, S. P. and Gelman, A. E. (1998). General methods for monitoring convergence  
529 of iterative simulations. *Journal of Computational and Graphical Statistics* **7**, 434–  
530 455.

531 Chalmers, A. (2008). *Temporal and spatial variability in coral condition at Sandy*  
532 *Bay, Ningaloo*. PhD thesis, The University of Western Australia.

533 Da-Silva, C. Q. (2006). Asymptotics for a population size estimator of a partially  
534 uncatchable population. *Annals of the Institute of Statistical Mathematics* **59**,  
535 603–615.

536 Da-Silva, C. Q., Rodrigues, J., Leite, J. G., and Milan, L. A. (2003). Bayesian es-  
537 timation of the size of a closed population using photo-id data with part of the  
538 population uncatchable. *Communications in Statistics - Simulation and Compu-  
539 tation* **32**, 677–696.

540 Holmberg, J., Norman, B., and Arzoumanian, Z. (2009). Estimating population size,  
541 structure, and residency time for whale sharks *rhincodon typus* through collabora-  
542 tive photo-identification. *Endangered Species Research* **7**, 39–53.

543 Link, W. A. and Barker, R. J. (2005). Modeling association among demographic  
544 parameters in analysis of open population capture-recapture data. *Biometrics* **61**,  
545 46–54.

546 Link, W. A., Yoshizaki, J., Bailey, L. L., and Pollock, K. H. (2010). Uncovering a  
547 latent multinomial: Analysis of mark-recapture data with misidentification. *Biometrika*  
548 **66**, 178–185.

549 Lukacs, P. M. and Burnham, K. P. (2005). Estimating population size from DNA-  
550 based closed capture-recapture data incorporating genotyping error. *Journal of*  
551 *Wildlife Management* **69**, 396–403.

552 Madon, B., Gimenez, O., McArdle, B., Scott Baker, C., and Garrigue, C. (2011). A  
553 new method for estimating animal abundance with two sources of data in capture-  
554 recapture studies. *Methods in Ecology and Evolution* **2**, 390–400.

555 Plummer, M. (2003). Jags : A program for analysis of bayesian graphical models  
556 using gibbs sampling jags. In *Proceedings of the 3rd International Workshop on*  
557 *Distributed Statistical Computing (DSC 2003)*, pages 1–10, Vienna, Austria.

558 Plummer, M. (2011). *rjags: Bayesian graphical models using MCMC*. R package  
559 version 3-5.

560 Plummer, M., Best, N., Cowles, K., and Vines, K. (2006). CODA: Convergence  
561 diagnosis and output analysis for MCMC. *R News* **6**, 7–11.

562 Team, R. D. C. (2012). *R: A Language and Environment for Statistical Computing*.  
563 R Foundation for Statistical Computing, Vienna, Austria. ISBN 3-900051-07-0.

564 Wilson, B., Hammond, P. S., and Thompson, P. M. (1999). Estimating size and  
565 assessing trends in a coastal bottlenose dolphin population. *Ecological Applications*  
566 **9**, 288–300.

567 Wright, J. A., Barker, R. J., Schofield, M. R., Frantz, A. C., Byrom, A. E., and

568 Gleeson, D. M. (2009). Incorporating genotype uncertainty into mark-recapture-  
569 type models for estimating abundance using DNA samples. *Biometrics* **65**, 833–40.

570 Yoshizaki, J., Brownie, C., Pollock, K. H., and Link, W. A. (2011). Modeling misiden-  
571 tification errors that result from use of genetic tags in capture-recapture studies.  
572 *Environmental and Ecological Statistics* **18**, 27–55.

573 Yoshizaki, J., Pollock, K. H., Brownie, C., and Webster, A. (2009). Modeling misiden-  
574 tification errors in capture-recapture studies using photographic identification of  
575 evolving marks. *Ecology* **90**, 3–9.

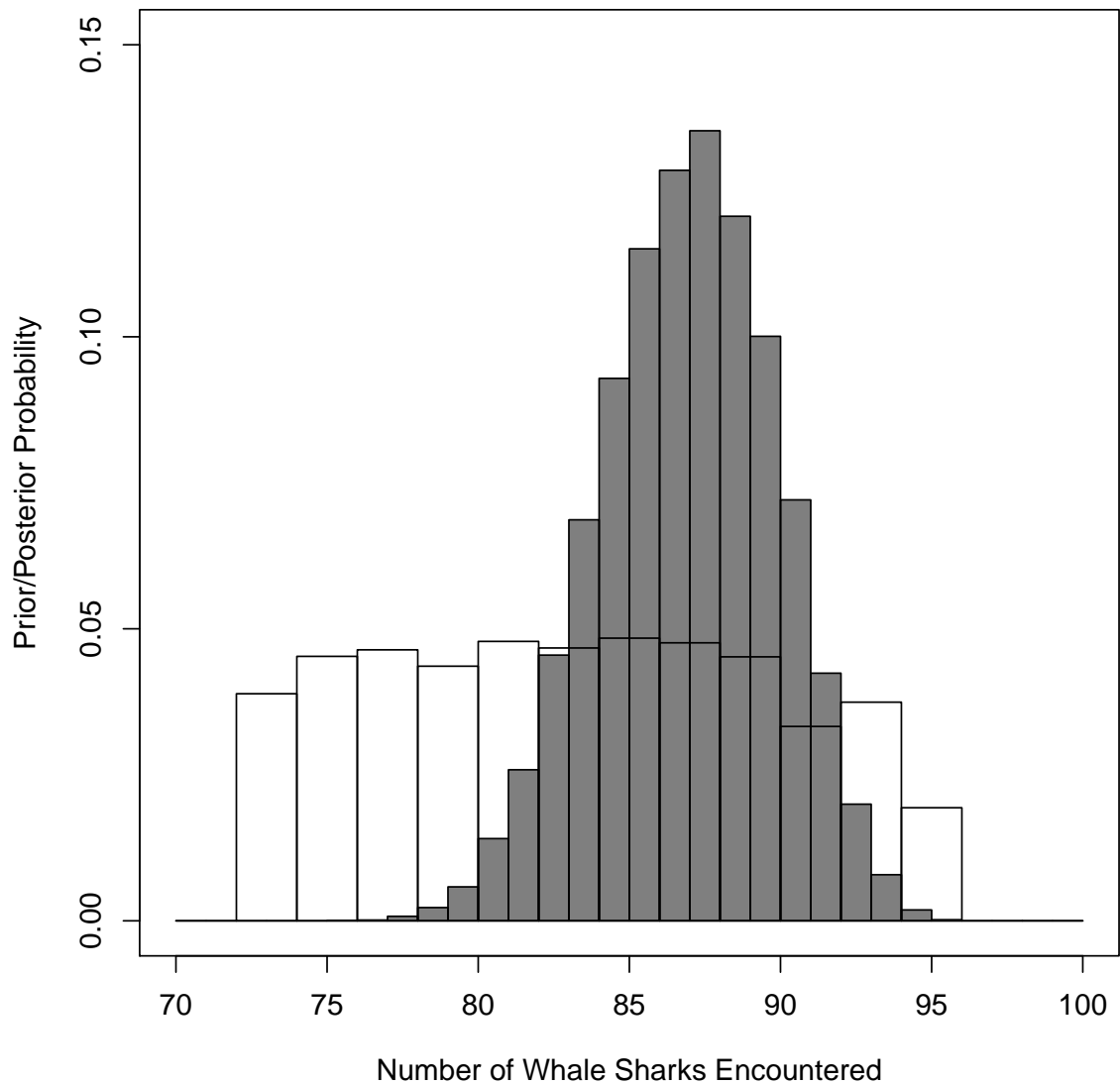


Figure 1: Comparison of the prior and posterior distribution of  $n^*$ . The prior distribution of  $n^*$  conditional on there being 170 observed capture histories is shown by the histogram with white bars. The posterior distribution of  $n^*$  is shown by the histogram with grey bars.

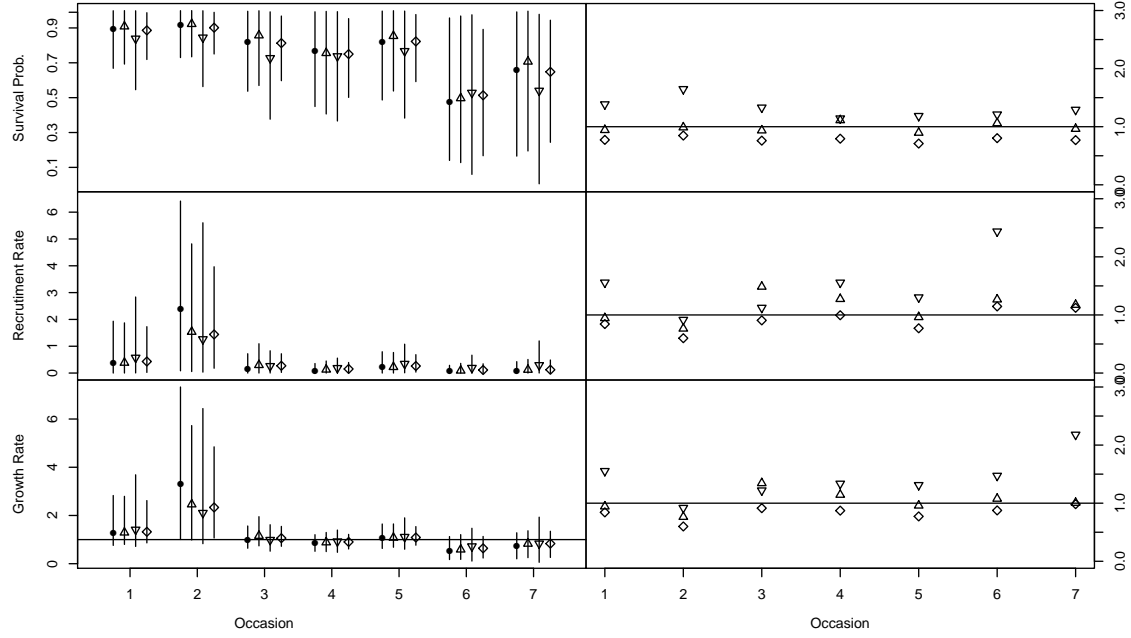


Figure 2: Comparison between the two-sided model and the three alternative models. The plots on the left-side of the figure compare the posterior means (points) and 95% credible intervals (vertical lines) of the survival probability (top), recruitment rate (middle), and population growth rate (bottom) obtained from the four models. The plots on the right side of the figure display the posterior standard deviations from the three alternative models relative to the posterior standard deviation from the two-sided model. Results from the two-sided model are represented by the circles, from the left-side photographs only by the upward pointing triangle, from the right-side photographs only by the downward pointing triangles, and from combined inference by the diamonds.

Table 1: Example of possible observed and true capture histories. Suppose that the data comprises the six observed histories given in the top of the table. The possible true histories that may have generated this data include these six plus the four additional histories in the bottom of the table.

	Occasion							
	1	2	3	4	5	6	7	8
1	0	0	L	0	L	0	0	0
2	0	0	0	0	L	0	0	0
3	0	0	R	0	0	0	0	0
4	0	0	0	R	R	0	0	0
5	0	0	S	B	R	0	0	0
6	S	0	S	0	0	0	0	0
7	0	0	B	0	L	0	0	0
8	0	0	B	0	L	0	0	0
9	0	0	L	R	B	0	0	0
10	0	0	0	R	B	0	0	0

Table 2: Performance of the estimates from the three simulation studies. Each column of the table presents the MSE of the posterior mean relative to the MSE of the posterior mean of the one-sided model, and the median width and estimated coverage probability of the 95% credible intervals for the survival probability ( $\phi$ ), recruitment rate ( $f$ ), and growth rate ( $\lambda$ ) for one of the three models – one-sided (OS), two-sided (TS), or combined-inference (CI). Descriptions of the models are provided in the text in Section 4.

		Simulation 1			Simulation 2			Simulation 3	
		OS	TS	CI	OS	TS	CI	OS	CI
$\phi$	MSE	1.00	.89	.87	1.00	.81	.81	1.00	1.00
	Width	.23	.20	.16	.30	.28	.21	.17	.12
	Cover	.97	.96	.90	.98	.99	.93	.95	.84
$f$	MSE	1.00	.88	.81	1.00	.86	.72	1.00	1.00
	Width	.35	.31	.24	.48	.42	.32	.26	.18
	Cover	.97	.95	.90	.99	.98	.96	.95	.84
$\lambda$	MSE	1.00	.88	.82	1.00	.86	.73	1.00	1.00
	Width	.41	.36	.29	.56	.50	.38	.31	.22
	Cover	.98	.97	.95	.99	.99	.97	.97	.87

Table 3: Posterior summary statistics for the demographic parameters  $\phi_k$ ,  $f_k$ ,  $\lambda_k$ , and  $p_k$  obtained from the two-sided model. The columns of the table provide posterior means followed with equal-tailed 95% credible intervals.

Occ ( $k$ )	Survival ( $\phi_k$ )	Recruitment ( $f_k$ )	Growth ( $\lambda_k$ )	Capture ( $p_k$ )
1	0.90(0.67,1.00)	0.36(0.00,1.93)	1.26(0.76,2.83)	0.23(0.08,0.43)
2	0.92(0.73,1.00)	2.40(0.08,6.41)	3.31(1.00,7.33)	0.19(0.05,0.33)
3	0.82(0.54,1.00)	0.17(0.00,0.72)	0.99(0.64,1.56)	0.26(0.15,0.43)
4	0.77(0.45,0.99)	0.09(0.00,0.36)	0.85(0.51,1.20)	0.22(0.13,0.34)
5	0.82(0.49,1.00)	0.23(0.00,0.79)	1.05(0.63,1.65)	0.22(0.12,0.36)
6	0.48(0.14,0.96)	0.06(0.00,0.29)	0.54(0.17,1.12)	0.25(0.14,0.42)
7	0.66(0.16,0.99)	0.09(0.00,0.42)	0.75(0.20,1.28)	0.20(0.06,0.37)
8	—	—	—	0.18(0.03,0.34)

Table 4: Posterior summary statistics for the conditional event probabilities.

Event ( $j$ )	Cond. Prob. ( $\rho_j$ )
1	0.29(0.20,0.38)
2	0.21(0.13,0.29)
3	0.45(0.36,0.54)
4	0.06(0.01,0.13)